Original Paper

Nucleation at cordierite glass surfaces: Kinetic aspects

Ralf Müller and Stefan Reinsch
Bundesanstalt für Materialforschung und -prüfung, Berlin (Germany)

Wolfgang Pannhorst
Schott Glaswerke, Mainz (Germany)

The surface nucleation of high-quartz solid solution crystals at fractured surfaces of glasses of the stoichiometric cordierite composition ($2MgO \cdot 2Al_2O_3 \cdot 5SiO_2$) was studied by optical microscopy. Particular attention was focused on the nucleation kinetics.

A constant nucleation density, $N \approx 10^{-4}\ \mu m^{-2}$, was found not to be significantly influenced by the time and the temperature of nucleation treatment. Even a very fast heating of samples employing heating rates up to 1200 K/min does not lower N substantially. However, for small average crystal diameters (<20 μm) a distribution of crystal size in the same order of magnitude is detectable indicating a simultaneous appearance of both measurable nucleation rates and growth velocities. It can be concluded that the surface nucleation of μ-cordierite occurs during the thermal treatment from a limited number of preferred nucleation sites; these sites are "used up" rapidly enough to cause a strong saturation effect of nucleation, but slow enough to cause a crystal size distribution at the same time.

The surface nucleation rate, I_S, was calculated from the observed distribution of crystal sizes. I_S progressively increases with rising temperature similar to the crystal growth velocity indicating a broad temperature range of essential nucleation activity. The latter must be regarded as the main obstacle to measure or to control surface nucleation density by means of two-step nucleation and growth treatments and must therefore be claimed to be mainly responsible for the observed constancy of N.

Keimbildung auf Cordieritglasoberflächen: Kinetische Aspekte

Die Kinetik der oberflächeninitiierten Keimbildung von Hochquarzmischkristallen („μ-Cordierit") auf Bruchflächen von Gläsern der Cordieritstöchiometrie ($2MgO \cdot 2Al_2O_3 \cdot 5SiO_2$) wurde mit Hilfe der optischen Mikroskopie untersucht.

Es wurde eine konstante Oberflächenkeimdichte von $N \approx 10^{-4}\ \mu m^{-2}$ gefunden. Ein signifikanter Einfluß von Zeit und Temperatur der Wärmebehandlung auf N war dabei nicht nachweisbar. Selbst ein schnelles Aufheizen der Proben mit bis zu 1200 K/min führte zu keiner deutlichen Verringerung von N. Andererseits wurde jedoch für den Fall kleiner Kristalldurchmesser (<20 μm) eine breite Streuung der Kristalldurchmesser in derselben Größenordnung gefunden, was darauf hinweist, daß Keimbildungsrate und Kristallwachstumsgeschwindigkeit gleichzeitig (d.h. im gleichen Temperaturbereich) meßbare Werte annehmen. Insgesamt kann gefolgert werden, daß die Keimbildung von μ-Cordierit zwar während der Wärmebehandlung erfolgt, jedoch auf eine begrenzte Anzahl keimbildender Defekte beschränkt ist. Der „Verbrauch" dieser Defekte erfolgt schnell genug, daß ein starker Sättigungseffekt resultiert, zugleich aber langsam genug, um eine Verteilung der Kristallgröße zu erlauben.

Aus der beobachteten Größenverteilung der Kristalle wurde die Oberflächenkeimbildungsrate I_S berechnet. I_S steigt – ähnlich der Kristallwachstumsgeschwindigkeit – mit wachsender Temperatur stetig an, was auf ein breites Temperaturintervall der Keimbildung hinweist. Dieser Effekt verhindert die Messung und Beeinflussung der Oberflächenkeimdichte mit Hilfe zweistufiger Keimbildungs- und Kristallwachstumsbehandlungen und ist somit auch für die beobachtete Konstanz der Oberflächenkeimdichte verantwortlich.

1. Introduction

Crystallization starts most readily from the glass surface if no volume nucleation has been promoted by adding nucleating agents to the glass composition. Despite the major scientific and technological importance arising from this fact, surface nucleation phenomena have gained much less attention than volume nucleation. The dominating factors that govern the kinetics of surface nucleation are still a matter of controversy.

On the one hand, the surface nucleation density, N, should be dominated by the time and the temperature of the nucleation treatment according to the classical nucleation theory as it has been well-confirmed by comprehensive studies of heterogeneous volume nucleation using noble metal substrates [1 and 2]. Analogous results were observed for the interface between a glass forming melt and a platinum crucible wall [3] or a platinum heating element [4]. Compared to the homogeneous nucleation, an enhanced nucleation rate at the platinum glass interface was observed particular at smaller undercoolings [3]. At "free" glass surfaces, evidence of a dominating influence of the time and the temperature of the nucleation treatment on the surface nucleation rate was reported by [5 to 8].

On the other hand, the surface condition has been observed more frequently to be the dominating factor that controls surface nucleation phenomena [4 and 9 to

Received January 10, revised manuscript March 23, 1995.

16]. A large scatter of N up to several orders of magnitude was brought about by different surface preparation techniques. Furthermore, the surface nucleation density was found not to be substantially influenced by the time and the temperature of the applied thermal nucleation treatment in [8 and 17 to 19]. Accordingly, surface nucleation was suggested to occur rapidly from a limited number of preferred nucleation sites reaching a saturation stage in a very short time. However, notwithstanding an unmeasurably high rate of depletion of active nucleation sites, the kinetics of using up these sites can cause a distribution of crystal sizes. This effect can be used to estimate the apparent surface nucleation rate by indirect means [20].

Altogether, it seems to depend on the rate of exhausting the given active nucleation sites whether the thermal nucleation treatment or the surface condition acts as the main controlling factor of surface nucleation phenomena. Accordingly, it was shown in [8] that the surface nucleation density of one crystalline phase, N_1, can be dominated by the thermal nucleation treatment while the surface nucleation density of another crystalline phase simultaneously growing from the same surface, N_2, is dominated by the surface condition.

Against that background, the influence of both the thermal nucleation treatment and different surface preparation techniques on the nucleation of high-quartz solid solution crystals at the surface of stoichiometric cordierite ($2MgO \cdot 2Al_2O_3 \cdot 5SiO_2$) glass was investigated. In the present paper, attention is focused on the nucleation kinetics and its experimental evidence. Investigations concerning the influence of different surface preparations on surface nucleation activity and the nature of active nucleation sites will be reported in a later publication.

2. Experimental

2.1. Specimens

Batches of nominal composition (in wt%) of cordierite 51.3 SiO_2, 34.9 Al_2O_3 and 13.8 MgO were melted at 1590 °C for 8 h in a platinum crucible. Glass plates of $\approx (10 \times 15 \times 1)$ cm^3 were prepared by casting the melts onto steel plates and cooling slowly to room temperature from 750 °C. Chemical analysis of the quenched glasses showed that no oxide component deviates more than 0.8 wt% from the nominal composition. Long-shaped glass bars ($(45 \times 5 \times 5)$ mm^3) were prepared by means of a diamond saw and were finished by SiC grinding. Subsequently, the bars were fractured in three-point bending under controlled load. Small glass cuboids of $(5 \times 5 \times 5)$ mm^3 with flat fractured surfaces of (5×5) mm^2 were thus obtained just before the beginning of the appropriate thermal treatment.

2.2. Thermal treatments

All thermal treatments were performed in free atmosphere. The accuracy of temperature measurement was about ±10 K. Isothermal treatments below 1100 °C were carried out in a conventional laboratory furnace. The samples were driven into the hot furnace using a platinum thermocouple as the sample holder. Short-time thermal treatments above 1100 °C and non-isothermal treatments were performed in a specially designed vertical tube furnace. The thermocouple and the platinum specimen holder were moved quickly along the tube axis, where a linear gradient of 20 K/cm between 300 and 1500 °C was maintained. Due to the small heat capacity of both the small samples and the platinum holder, very high heating rates up to about 1200 K/min were attained, at least in the vicinity of the glass surface.

2.3. Nucelation density measurement

The surface nucleation density, N, was determined by optical microscopy. Single crystallites of 3 µm or more in diameter were detectable. To discriminate single crystallites, the nearest neighbour distance between two crystallites, $2\,l$, had to be larger than 3 µm. The corresponding upper limit of the surface nucleation density, N_{max}, can be roughly estimated from $2\,l$ assuming that, on the average, each nucleus is surrounded by an area of about $(2\,l)^2$. Consequently, $N_{max} = 1/(2\,l)^2 = 1/(3\ \mu m)^2 \approx \approx 10^{-1}\ \mu m^{-2}$ results. The lower limit of N, N_{min}, is due to the fact that at least a few nuclei must be present at the limited area of the glass surface. Thus, in order-of-magnitude accuracy, N_{min} of $10^{-8}\ \mu m^{-2}$ corresponds to the occurrence of one crystal per (5×5) mm^2.

3. Theoretical background

Surface nucleation can be treated in terms of the classical nucleation theory as a heterogeneous nucleation phenomenon. Comprehensive reviews of the theory of heterogeneous nucleation have been presented in [21 and 22]. For the sake of a more transparent discussion of the results given in the sections 4. and 5., some basic equations from [21 and 22] are briefly summarized in this section.

3.1. Influence of temperature

The influence of the temperature, T, on the nucleation rate is basically related to the work $W(T)$ needed to form a crystalline cluster within the parent liquid. $W(T)$ results from the balance of the molar free enthalpy surplus of crystallization, $\Delta\mu(T)$, and the energy amount required to form the crystal/liquid interface owning the specific surface free energy, σ. While subcritical crystalline clusters (embryos) tend to be redissolved, the stable supercritical clusters (nuclei) tend to grow further. Neglecting any kinetic effects, the steady-state nucleation rate, $I_0(T)$, results from the number of crystalline clusters surpassing the critical size per unit time:

$$I_0(T) \approx \text{const}\,\frac{1}{\eta(T)}\exp\left(\frac{W_c(T)}{k\,T}\right) \qquad (1)$$

$$\text{with}\quad W_c(T) = \text{const}\,\frac{\sigma^3}{\Delta\mu(T)^2}\,.$$

$W_c(T)$ is the work to form a critical nucleus and $\eta(T)$ is the bulk viscosity; at low temperatures $I_0(T)$ is limited by the viscosity-related diffusion rate while at high temperatures $I_0(T)$ is limited by $\Delta\mu(T)$ that is steadily increasing with decreasing temperature below the melting point. Hence, the nucleation rate passes through a maximum at some intermediate temperatures.

Referring to heterogeneous nucleation, a low specific free surface energy at the crystal/substrate interface, σ^*, is assumed to reduce $W_c(T)$. This is usually described by introducing a dimensionless factor, $\Phi(\Phi < 1)$, that does not depend on temperature:

$$W_c^*(T) = W_c(T) \cdot \Phi \,. \tag{2}$$

Hence, a quite analogous temperature dependence is to be expected for both homogeneous and heterogeneous nucleation rates. However, the heterogeneous nucleation rate, $I_0^*(T)$, should be considerably higher than $I_0(T)$ particular at small undercoolings where $W_c^*(T)$ is dominating in equation (1). At large undercoolings the domination of the viscosity prevents an essential enlargement of $I_0^*(T)$. Thus, a low value of Φ broadens the temperature interval of essential nucleation activity particular to higher temperatures.

3.2. Influence of time

The apparent nucleation rates, $I(T, t)$, derived from experiments, do not always reach the corresponding steady-state value, $I_0(T)$. Two reasons can be responsible for this observation: a) the non-steady-state character of nucleation and b) overall kinetic saturation effects.

a) When the temperature of the melt is changed, a non-steady-state time lag, $\tau(T)$, is required to establish a new stationary equilibrium size distribution of subcritical crystalline clusters before $I(T, t)$ can attain $I_0(T)$. This effect may be sufficiently well approximated as:

$$I(T, t) = I_0(T) \exp(-\tau(T)/t) \tag{3}$$

b) The overall kinetics of surface nucleation might be divided into three distinct cases that all may contribute to the apparent nucleation density. In figure 1 the features of these specific cases are schematically exemplified.

First case: Generally, every point, even on a pristine glass/vacuum interface, might be considered to be able to promote surface nucleation during appropriate nucleation treatment. This "intrinsic" surface nucleation rate, $I_i(T, t)$, causes a surface nucleation density, N_i, that is dominated by the time t and temperature T of the nucleation treatment (figure 1, curve 1):

$$N_i(T, t) = \int_0^t I_i(T, \xi)\, d\xi \,. \tag{4}$$

No kinetic saturation effect is caused until the nucleation is impeded due to crystal growth in this case.

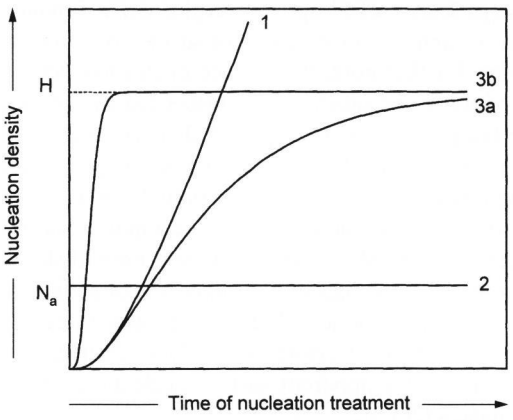

Figure 1. Schematic of overall surface nucleation kinetics. Curve 1: "intrinsic" surface nucleation according to equation (4); curve 2: "athermal" surface nucleation; curves 3a and b: "site-controlled" surface nucleation according to equation (5) for low (curve 3a) and high (curve 3b) nucleation rates at active sites.

Second case: On the other hand, it might be assumed that nuclei had been generated already during the surface preparation, for instance due to strong local mechanical damaging at low ambient temperatures. This "athermal" nucleation density, N_a, would not be altered by any subsequent thermal treatment. In contrast to N_i, N_a is dominated by the surface preparation technique only (figure 1, curve 2).

Third case: Finally, surface nucleation can be considered to occur during the thermal nucleation treatment restricted to a limited number of uniform active nucleation sites. This "site-controlled" surface nucleation density, $N_S(T, t)$, depends on both the number of these active sites H per unit square and the nucleation rate, $I_S(T, t)$, at these active sites according to:

$$N_S(T, t) = H \cdot \left[1 - \exp\left(-\int_0^t I_S(T, \xi)\, d\xi\right)\right]. \tag{5}$$

To avoid confusion, it is necessary to distinguish the nucleation rate at the active sites, $I_S(T, t)$, from the apparent "site-controlled" surface nucleation rate, $dN_S(T, t)/dt$, that is proportional to the number density of active sites not "used up" so far:

$$dN_S(T, t)/dt = [H - N_S(T, t)] \cdot I_S(T, t) \,. \tag{6}$$

For low values of $I_S(T, t)$ no evident saturation effect is caused before the nucleation is impeded by crystal growth. $N_S(T, t)$ remains much smaller than H and $dN_S(T, t)/dt \approx I_S(T, t) \cdot H$ is valid. H remains unknown during this initial nucleation stage because no saturation level is attained. Accordingly, $I_S(T, t) \cdot H$ can easily be misinterpreted as $I_i(T, t)$, which could lead up to somewhat confusion in thermodynamical calculations based on these data (figure 1, curve 3a). When $I_S(T, t)$ reaches its steady-state value $I_{S0}(T)$ (see equation (3)) during

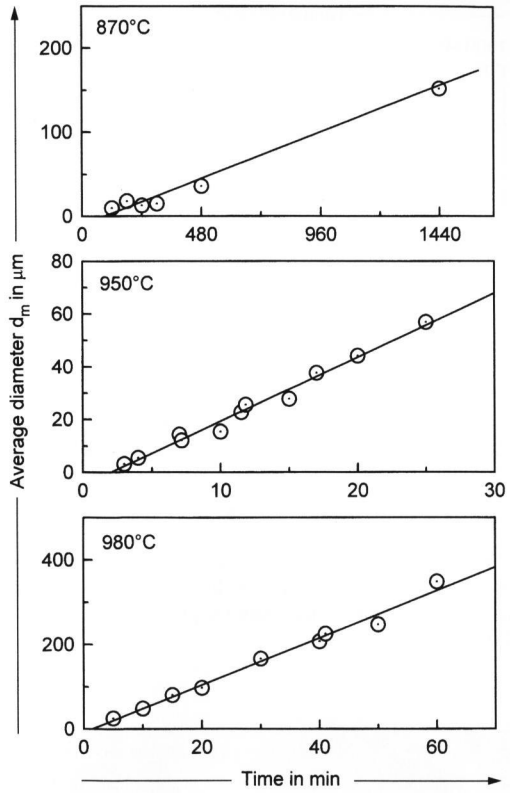

Figure 2. Average diameter of μ-cordierite surface crystals as a function of time at different temperatures. A small delay of the observed linear growth indicates the appearance of a non-steady-state time lag of nucleation.

the initial stage already, a "steady-state" value of the apparent "site-controlled" surface nucleation rate, $dN_{S0}(T)/dt$, will be attained:

$$dN_{S0}(T)/dt \approx H \cdot I_{S0}(T) \; . \qquad (7)$$

For high values of $I_S(T, t)$ the active nucleation sites are used up very rapidly at least before any crystallite will grow up to a detectable size. After the depletion of all nucleation sites a saturation stage at $N_S(T, t) = H$ is reached (figure 1, curve 3b). Thus, $I_S(T, t)$ is unmeasurably high and it is impossible to distinguish the "site-controlled" nucleation mechanism from the "athermal" one (figure 1, curves 3b and 2).

4. Results

4.1. X-ray measurements

X-ray measurements were performed in order to ensure that the surface nucleation data discussed in the following sections are related to the same crystalline phase. According to [23], it was found that the primary crystalline phase consists of metastable high-quartz solid solution crystals referred to as μ-cordierite in the following. Although this phase rapidly transforms into the high-temperature polymorph of cordierite at temperatures above 1000 °C, μ-cordierite is detectable as the primary phase even up to 1300 °C by means of short-time thermal treatments. The (101)-interplanar spacing, d_{101}, was found to be (0.345 ± 0.001) nm in all cases. This value is close to 0.344 nm calculated from the cell dimensions given in [23] for high-quartz solid solution crystals of the cordierite stoichiometry. The d_{101} value of pure high-quartz is 3.37 nm (calculated from the corresponding cell dimension data given in [23]). It can be inferred that the chemical composition of μ-cordierite does not essentially differ from the cordierite stoichiometry of the parent glass. The latter result well agrees with ESCA measurements of the chemical composition of μ-cordierite crystals grown at 870 and 1000 °C within the spatial resolution and accuracy.

4.2. Crystal growth velocity

For the sake of reproducible surface nucleation density measurements, small but well-detectable surface crystals are required. For that reason the influence of temperature on the crystal growth velocity of μ-cordierite was studied by optical microscopy between 850 and 1350 °C.

In figure 2 the average diameter of single μ-cordierite crystals is plotted against the time for various temperatures. The crystal growth velocity is independent of time suggesting an interface-controlled growth mechanism where long-range diffusion processes of single chemical components are not necessary. This mechanism is usually encountered when the chemical composition of the crystal phase does not essentially differ from that of the melt. Figure 2 shows a small delay of linear crystal growth from 1 up to 80 min for temperatures between 980 and 870 °C. This effect indicates the appearance of a non-steady-state time lag of the surface-induced nucleation of μ-cordierite.

The temperature dependence of the crystal growth velocity is given in figure 3. The average diameter of isolated crystallites and the thickness of the crystalline surface layer were measured at temperatures below 920 and above 980 °C, respectively. Between these temperatures both methods were used simultaneously. Most data in figure 3 are related to large crystals (see for example figure 4a in comparison to figure 4b). In this case, an almost uniform crystal size is evident and the corresponding mean radius of single crystallites is quite similar to the thickness of the crystalline surface layer.

A maximal crystal growth velocity of about 600 µm/min is reached at 1250 °C. The straight line on the low-temperature side was fitted according to the Arrhenius law with

$$dr(T)/dt = 3 \cdot 10^{17} \exp(-415 \text{ kJ}/(R\,T)) \text{ µm/min}.$$

No data for temperatures above 1350 °C are presented due to the progressive occurrence of mullite crystals and the compositional change of the melt which is expected for this situation. However, the crystal growth velocity will be zero, at the very least, at the melting point of the stable high-temperature polymorph of cordierite (melting temperature ≈ 1467 °C, arrow in figure 3 [24]).

4.3. Nucleation density

The nucleation density of μ-cordierite crystals, N, at fractured glass surfaces heat-treated isothermally at various temperatures is shown in figure 5 as a function of time. N was found to be about 10^{-4} µm^{-2} within an order-of-magnitude accuracy. Despite the large scatter of N, no systematic influence of the thermal treatment either in time or temperature is evident. Even preliminary heat treatments up to 310 h at temperatures between 100 and 860 °C do not influence N as demonstrated in [8] for mechanically polished surfaces of the glasses used in the present investigation. It must be inferred that nucleation of μ-cordierite at fractured cordierite glass surfaces appears either as an "athermal" phenomenon (figure 1, curve 2) or as a "site-controlled" surface nucleation occurring from a limited number of preferred nucleation sites which have been completely exhausted during the first stage of the thermal treatment (figure 1, curve 3b).

In case of an "athermal" surface nucleation even a very fast running over the whole temperature range of essential nucleation activity would not alter the apparent surface nucleation density. Therefore, fractured cordierite glass samples were rapidly heated up to temperatures between 990 and 1130 °C. High heating rates up to 1200 K/min were applied. The upper temperature limit was carefully tuned to the applied heating rate in order to ensure an average crystal diameter of about 10 µm for all experiments.

The results are given in figure 6. With increasing heating rate the surface nucleation density, N, tends to decrease. While this effect is somewhat obscured by the large scatter of N at fractured surfaces, it is more pronounced at polished surfaces indicating a "site-controlled" nucleation phenomenon. Nevertheless, the observed slight decrease in final nucleation density is restricted to very high heating rates of about 1000 K/min due to a very strong saturation effect. Two alternative causes may be responsible for that strong saturation effect. On the one hand, an unmeasurably high nucleation rate and an unmeasurably short non-steady-state time lag of nucleation can be regarded to cause the almost complete depletion of active sites. On the other hand, the range of essential nucleation activity can be broadened even up to 1100 °C due to a very low value of the nucleation activity Φ in equation (2). Accordingly, a full saturation of active sites can be accomplished at rather high annealing temperatures for much lower nucleation rates.

4.4. Crystal size distribution

If the latter is true and a measurable crystal growth velocity occurs at temperatures of evident nucleation activity, crystals nucleated earlier than others will grow up to larger diameters. Notwithstanding an almost complete depletion of active nucleation sites, the corresponding depletion kinetics would cause a size distribution of the

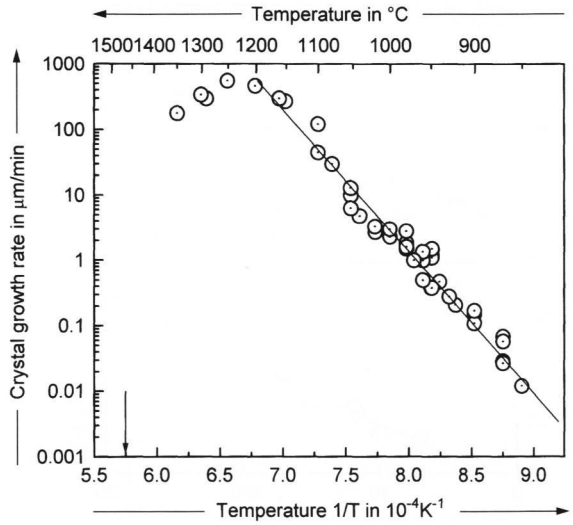

Figure 3. Temperature dependence of the crystal growth velocity of μ-cordierite. The arrow indicates the melting temperature of the stable high-temperature polymorph of cordierite at 1467 °C [24].

a) 100 µm

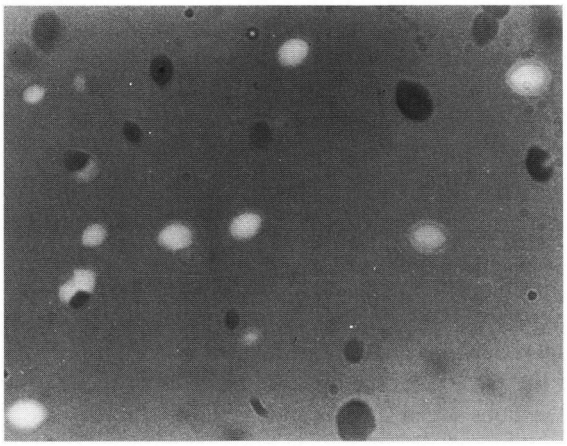

b) 50 µm

Figures 4a and b. μ-cordierite crystals nucleated at fractured glass surfaces. Transmitting optical micrographs, top view under slightly crossed nicols; a) 30 min at 960 °C, b) 10 min at 950 °C.

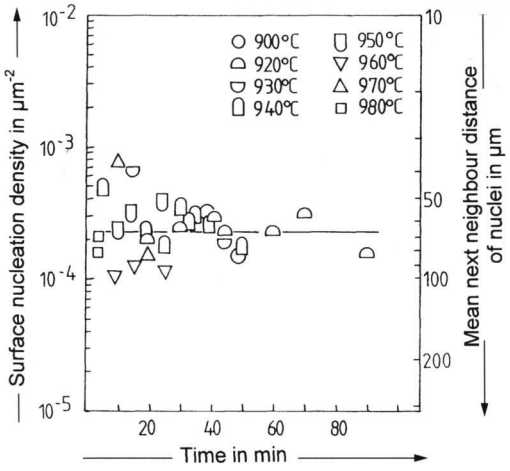

Figure 5. Nucleation density at fractured cordierite glass surfaces annealed at different temperatures in free atmosphere as a function of time. The right ordinate denotes the corresponding mean next neighbour distance of two surface nuclei, $2\,l$ (see section 2.3.).

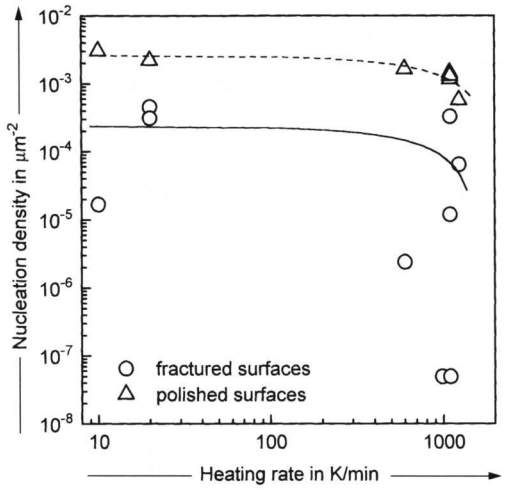

Figure 6. Nucleation density at fractured cordierite glass surfaces heated up with different heating rates to different holding temperatures.

surface crystallites this way [20]. A maximal deviation of different crystal diameters, $\Delta d(T)$, would appear due to the "saturation" time, $\Delta t_S(T)$, required to use up all given nucleation sites ($\mathrm{d}r(T)/\mathrm{d}t$ is the crystal growth velocity):

$$\Delta d(T) = \Delta t_S(T) \cdot 2\,\mathrm{d}r(T)/\mathrm{d}t\,. \tag{8}$$

Confirming similar results reported in [20], such a size distribution is detectable for low average crystal diameters $d_M(T, t) < 20$ µm. The results are given in figure 7 in terms of the relative number of surface crystallites belonging to different classes of crystal diameters. A maximum deviation of the crystal diameter, $\Delta d(T)$, up to ≈ 24 µm surpassing the mean crystal diameter was observed (see also figure 4b). Consequently, it can be excluded that the crystal growth morphology of differently orientated crystals has strongly affected the results. When the time of the thermal treatment becomes larger than $\Delta t_S(T)$, a prolonged thermal treatment yields an average crystal diameter, $d_M(T, t)$, much larger than the nucleation-induced size variation $\Delta d(T)$. Accordingly, an almost uniform crystal size distribution was observed for large average values of the crystal size (figure 4a).

Following the approach as already outlined, figure 7 gives clear evidence that the nucleation of μ-cordierite occurs at temperatures of detectable crystal growth velocity (which is in contrast to any athermal nucleation phenomenon). Accordingly, the saturation stage of nucleation is not reached until the crystals have grown up to a detectable size. Hence, the strong saturation effect (indicated by figure 6) is not simply caused by a very rapid depletion of active nucleation sites within a small temperature interval of nucleation activity at low temperatures. Instead of this, it must be inferred that the nucleation rate is considerably large even at high temperatures up to 1050 °C. The maximum crystal size deviation, $\Delta d(T)$, was found not to be very sensitive to the temperature. The value of $\Delta d(T)$ lies in the range of 11 to 24 µm for the four temperatures investigated here and seems to pass through a smooth maximum at about 950 °C. For that reason, a similar temperature dependence of both the surface nucleation and the crystal growth velocity of μ-cordierite may be anticipated.

5. Discussion

Based on crystal growth rate data (figure 3), the depletion kinetics of μ-cordierite were calculated from the observed size distribution (figure 7). The level of depletion of the given active nucleation sites, $N(T, t)/H$, is plotted against the time in figure 8 (points). The "saturation" time, $\Delta t_S(T)$, which is necessary to complete the depletion of active nucleation sites ranges from 100 down to 0.7 min at temperatures between 870 and 1050 °C.

The nucleation rate at the given active nucleation sites, $I_S(T, t)$, was calculated from equation (5) using the data shown in figure 8 (points). The non-steady-state character of $I_S(T, t)$ was described according to equation (3). With respect to equation (3), equation (5) yields on integration [21]:

$$N_S(T, t) = H \cdot \{1 - \exp[-I_{S0}(T) \cdot t \cdot C(T, t)]\} \tag{9}$$

$$\text{with } C(T, t) = \exp[-\tau(T)/t] + [\tau(T)/t] \cdot \mathfrak{Ei}[-\tau(T)/t]\,.$$

The exponential integral, $\mathfrak{Ei}[-\tau(T)/t]$, was numerically approximated according to [25]. The best-fitted curves of the level of saturation, $N_S(T, t)/H$, are shown in figure 8 (solid lines).

5.1. Temperature dependence

The fitted values of the steady-state surface nucleation rate, $I_{S0}(T)$ and the non-steady-state time lag $\tau(T)$, are plotted against temperature in figure 9. Values of $\tau(T)$ up to 40 min at 870 °C were obtained strongly decreasing

with rising temperature. These values roughly confirm the delay of linear crystal growth found in crystal growth measurements (figure 2). The value of $\tau(T)$ becomes smaller than 1 min beyond 1000 °C. $I_{S0}(T)$ steadily increases with increasing temperature up to 13 min^{-1}. No temperature maximum of $I_{S0}(T)$ was found up to 1050 °C (more than 200 K above T_g). A further increase of $I_{S0}(T)$ with increasing temperature might be reasonably expected causing a very broad temperature range of essential nucleation activity at high temperatures.

The latter indicates a very low value of Φ in equation (2). As illustrated in figures 3 and 9, a large nucleation rate can occur simultaneously with a considerable growth velocity of μ-cordierite in this case. Consequently, almost any thermal treatment, allowing a sufficient growth of μ-cordierite crystals, probably yields a full depletion of all given active nucleation sites. This effect must be considered to be the main obstacle for both a successful study and a technological control of the apparent surface nucleation density by means of conventional two-step nucleation and growth treatments.

5.2. Numerical values

For the sake of a comparison with surface nucleation data reported in previous literature, the apparent surface nucleation rate, $dN_S(T, t)/dt$, was calculated from equation (5) based on the values of $I_{S0}(T)$ shown in figure 9 and the number density of active nucleation sites $H \approx 10^{-4}$ μm^{-2} estimated from figure 5. The maximal values of the apparent surface nucleation rate, $(dN_S(T, t)/dt)_{max}$, which were found to occur at some medium saturation stages, $t \approx \tau(T)$, for all temperatures investigated here, are shown by curve 5 in figure 10 (points ◇). The solid points of curve 5 (◆) were calculated from $dN_S(T, t)$ data for mechanically polished surfaces of glass of the cordierite composition [20], where a quite similar value of H was reported. $(dN_S(T, t)/dt)_{max}$ ranges from $5 \cdot 10^{-8}$ up to $3.4 \cdot 10^{-4}$ μm^{-2} min^{-1}, an interval that comprises the data in figure 10, which are directly measured (curves 1 to 4). Besides the $(dN_S(T, t)/dt)_{max}$ values, that are more or less influenced by the saturation effect, one might compare the respective values of $H \cdot I_{S0}(T)$ (see equation (7)) to other literature data. $H \cdot I_{S0}(T)$ can be easily estimated from figure 9 by multiplying the data of $I_{S0}(T)$ with $H = 10^{-4}$ μm^{-2}. The resulting values (points ◇) range from $3.8 \cdot 10^{-6}$ up to $1.3 \cdot 10^{-3}$ μm^{-2} min^{-1}.

It should be emphasized, however, that the apparent "site-controlled" surface nucleation rate depends on the final saturation stage, H, that is strongly affected by the surface condition. The latter has been widely accepted to play a crucial role in surface nucleation indicating "site-controlled" nucleation phenomena. A strong influence of the surface condition was also reported for the nucleation data shown in curves 1 [5], 3 [7] and 4 [26]. Therefore, it is difficult to compare the surface nucleation data summarized in figure 10 among each other without careful consideration of surface conditions and the knowledge of the respective H values. Unfortunately, no saturation effect was reported in [6] for the nucleation data shown in curve 2 preventing an estimation of the corresponding value of H. For the surface nucleation data shown in curve 4 [26] a saturation stage depending on the temperature was observed. In case of curve 3 [7] a saturation stage was found only at temperatures above 850 °C.

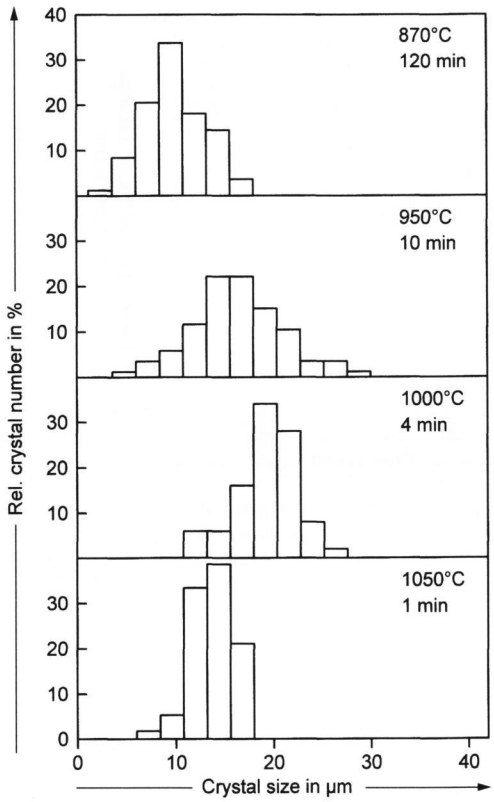

Figure 7. Frequency distribution of the size of μ-cordierite crystals nucleated at fractured cordierite glass surfaces for different temperatures and times.

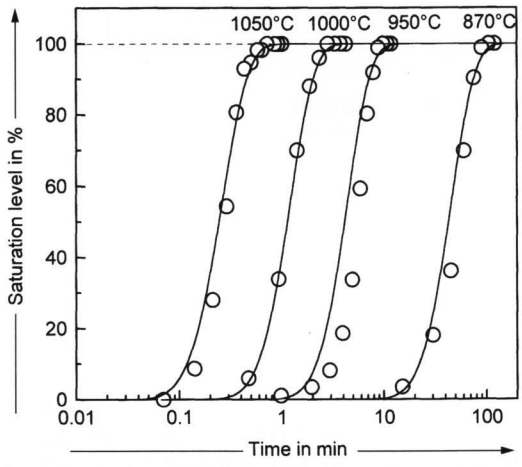

Figure 8. Level of saturation of active nucleation sites as a function of time at different temperatures. Points calculated from figure 7 according to equation (9), fitted curves according to equations (3 and 5).

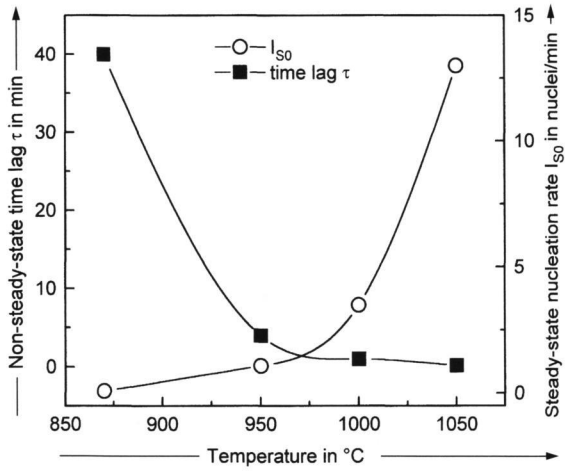

Figure 9. Non-steady-state time lag, $\tau(T)$, and steady-state nucleation rate, $I_{S0}(T)$, values derived from figure 8 as a function of temperature.

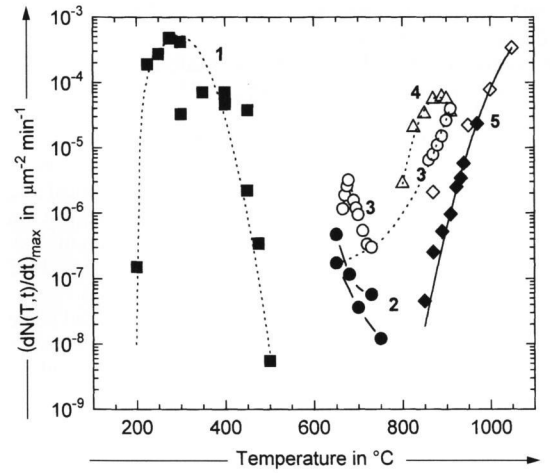

Figure 10. Kinetic surface nucleation data for "free" glass surfaces. Curve 1: $Na_2Si_2O_5$ crystals at fire-polished surfaces of $Na_2O \cdot 2SiO_2$ glass [5]; curve 2: $Na_2O \cdot 2CaO \cdot SiO_2$ crystals at fire-polished surfaces of $57SiO_2 \cdot 21Na_2O \cdot 21CaO$ glass [6]; curve 3: cristobalite crystals at fire-polished surfaces of float glass [7]; curve 4: X-phase crystals at polished surfaces of cordierite glass ($2MgO \cdot 2Al_2O_3 \cdot 5SiO_2$) [26], curve 5: μ-cordierite at fractured (◇, this work) and mechanically polished (◆) [20] surfaces of cordierite glass.

A discussion of the kinetic surface nucleation data in terms of the thermodynamic concept briefly outlined in section 3. suffers from another problem. In using equation (5), infinite small active nucleation sites (points) are implicitly assumed leading to the physically uniformative unit (number of nuclei per minute) of $I_{S0}(T)$. For the sake of comparison of surface nucleation data among each other, it would be better to introduce a substrate/melt interface area into equation (5). A surface nucleation rate at the substrate/melt interface would be calculable depending on the nucleation activity Φ of the given kind of active sites this way. Unfortunately, even then the interface area of active nucleation sites will probably remain unmeasurable in most cases making it difficult to compare experimental nucleation data with those calculated according to the classical nucleation theory at all.

6. Summary

A constant surface nucleation density, N, of μ-cordierite of about 10^{-4} μm^{-2} was found at fractured surfaces being not substantially influenced by time or temperature of the applied isothermal thermal treatment. Even preliminary heat treatment up to 310 h at temperatures between 100 and 860 °C do not promote surface nucleation of μ-cordierite as has been reported by [8]. Additionally, a very fast heating of samples, employing heating rates up to 1200 K/min, do not reduce N substantially. However, for small average crystal diameters (<20 μm) a distribution of crystal sizes of the same order of magnitude is detectable indicating a simultaneous appearance of both measurable nucleation and growth velocity.

Summing up, surface nucleation of μ-cordierite must be regarded as occurring from a limited number of preferred nucleation sites with a nucleation rate which is fast enough to cause an almost complete saturation during all thermal treatments applied here and which is small enough to cause a measurable crystal size distribution within the wide temperature range from 870 up to 1050 °C. This is due to the fact that the nucleation rate is progressively increasing with rising temperature up to 1050 °C (similar to the rate of crystal growth) due to a very broad temperature interval of essential nucleation activity. The latter must be considered as the main obstacle to both measure and control the nucleation density by means of conventional two-step nucleation and growth treatments.

*

The authors thank D. Thamm for his interest and valuable help in this study and K. Tews for technical assistance. The investigations presented here are part of a co-operative effort of the Technical Committee 7 of the ICG to advance the understanding of surface nucleation; discussions with I. Donald, W. M. Fokin, K. Heide, W. Höland, T. Kokubo, G. Völksch, I. Szabo, and E. D. Zanotto are gratefully acknowledged. S. Reinsch acknowledges the financial support by Schott Glaswerke, Mainz (Germany).

7. Nomenclature

7.1. Symbols

C	reduction of the term: $\exp[-\tau(T)/t] + [\tau(T)/t] \cdot \mathrm{ei}[-\tau(T)/t]$
d	diameter of surface crystals
d_M	average diameter of surface crystals
$\mathfrak{Ei}$	exponential integral
H	number density of active nucleation sites
I	surface nucleation rate
I_S	rate of using up active nucleation sites
$2l$	mean nearest neighbour distance between two crystallites
N	surface nucleation density

r	average radius of surface crystals or thickness of crystalline surface layer
t	time
Δt_S	"saturation" time, time that is necessary to complete the depletion of active nucleation sites
T	temperature
W	work needed to form a crystalline cluster within the parent liquid
η	bulk viscosity
$\Delta\mu$	molar free enthalpy surplus of crystallization
ξ	time
σ	specific surface free energy
τ	non-steady-state time lag
Φ	dimensionless factor, "activity" of nucleation site

7.2. Subscripts

a	related to "athermal" surface nucleation
c	related to critical nucleus
i	related to "intrinsic" surface nucleation
max	maximal value
min	minimal value
S	related to "site-controlled" surface nucleation
0	steady-state value

7.3. Superscript

*	related to heterogeneous nucleation

8. References

[1] Gutzow, I.: Induced crystallisation of glass-forming systems: a case of transient heterogeneous nucleation. Pt. 1 and 2. Contemp. Phys. **21** (1980) p. 121–137, 243–263.

[2] González-Oliver, C. J. R.; James, P. F.: Influence of platinum and silver additions on crystal nucleation in glasses near the $Na_2O \cdot 2CaO \cdot 3SiO_2$ composition and in other soda–lime–silica glasses. In: Simmons, J. H.; Uhlmann, D. R.; Beall, G. H. (eds.): Nucleation and crystallization in glasses. Columbus, OH (USA): Am. Ceram. Soc. 1982. p. 49–65. (Advances in Ceramics. Vol. 4.).

[3] Burnett, D. G.; Douglas, R. W.: Nucleation and crystallisation in the soda–baria–silica system. Phys. Chem. Glasses **12** (1971) no. 5, p. 117–124.

[4] Scott, W. D.; Pask, J. A.: Nucleation and growth of sodium disilicate crystals in sodium disilicate glass. J. Am. Ceram. Soc. **44** (1961) no. 4, p. 181–187.

[5] Takahashi, K.; Sakaino, T.: Influence of atmospheres on the surface crystallization of $Na_2O–2SiO_2$ glass. Bull. Tokyo Inst. Technol. **104** (1971) p. 1–26.

[6] Strnad, Z.; Douglas, R. W.: Nucleation and crystallisation in the soda–lime–silica system. Phys. Chem. Glasses **14** (1973) no. 2, p. 33–36.

[7] Deubener, J.; Brückner, R.; Hessenkemper, H.: Nucleation and crystallization kinetics on float glass surfaces. Glastech. Ber. **65** (1992) no. 9, p. 256–266.

[8] Yuritsin, N. S.; Fokin, V. M.; Kalinina, A. M. et al.: Nucleation and growth of crystals at the surface of glass of the composition $2MgO–2Al_2O_2–5SiO_2$. In: Proc. National Conference on the Glassy State, Leningrad (Russia) 1986. p. 235–236.

[9] Tabata, K.: On the causes of the surface devitrification of glasses. J. Am. Ceram. Soc. **10** (1927) no. 1, p. 6–22.

[10] Swift, H. R.: Some experiments on crystal growth and solution in glasses. J. Am. Ceram. Soc. **30** (1947) no. 6, p. 165–169.

[11] Ernsberger, F. M.: A study of the origin and frequency of occurrence of Griffith microcracks on glass surfaces. In: Advances in glass technology. Tech. papers of VI International Congress on Glass, Washington, DC (USA) 1962. New York: Plenum Press 1962. p. 511–524.

[12] Booth, C. L.; Rindone, G. E.: Surface nucleation of glass fibers. In: Advances in glass technology. Pt. 2. History papers and discussions of technical papers of VI International Congress on Glass, Washington, DC (USA) 1962. New York: Plenum Press 1963. p. 42–43.

[13] Bergeron, C. G.; De Luca, J. P.: Crystal growth at bubble surfaces in glass. J. Am. Ceram. Soc. **50** (1967) no. 2, p. 116–117.

[14] Müller, G.: Oberflächengesteuerte Kristallisation von Glas – ein Weg zur Herstellung neuer Werkstoffe. Fortschr. Mineralog. **58** (1980) no. 1, p. 68–78.

[15] McMillan, P. W.: The crystallisation of glasses. J. Non-Cryst. Solids **52** (1982) p. 67–76.

[16] Zanotto, E. D.: Experimental studies of the surface nucleation and crystallization of glasses. In: Weinberg, M. C. (ed.): Nucleation and crystallization in liquids and glasses. International Symposium, Mountain Stone, AL (USA) 1992. Westerville, OH: Am. Ceram. Soc. 1993. p. 65–74. (Ceram. Trans. Vol 30.)

[17] Zanotto, E. D.; Basso, R.: Cristalização superficial em vidros-mecanismo. Cerâmica **32** (1986) no. 197, p. 117–120.

[18] Zanotto, E. D., São Carlos (Brasil): Pers. commun.

[19] Heide, K.; Völksch, G.; Hanay, C.: Characterization of crystallisation in cordierite glasses by means of optical and electron microscopy. In: XVI International Congress on Glass, Madrid 1992. Vol. 5. Madrid: Soc. Esp. Ceram. Vid. 1992. p. 111–116. (Bol. Soc. Esp. Ceram. Vid. 31-C (1992) 5.)

[20] Fokin, V. M.; Yuritsin, N. S.; Kalinina, A. M. et al.: The temperature dependence of the μ-cordierite crystals nucleation rate on the polished surface of cordierite glass. In: Rüssel, C. (ed.): Proc. 5th International Otto Schott Colloquium, Jena 1994. Frankfurt/M.: Verl. Dtsch. Glastech. Ges. 1994. p. 392–395. (Glastech. Ber. Glass Sci. Technol. 67C (1994).)

[21] Toschev, S.; Gutzow, I.: Nichtstationäre Keimbildung: Theorie und Experiment. Krist. Tech. **7** (1972) p. 43–73.

[22] Gutzow, I.; Penkov, I.: Nucleation catalysis in glass-forming melts: principal methods, their possibilities and limitations. In: 3. Internationales Otto-Schott-Kolloquium, Jena 1986. p. 907–919. (Wiss. Z. Fried.-Schiller-Univ. Jena, Naturwiss. R. **36** (1987) no. 5/6.)

[23] Schreyer, W.; Schairer, J. F.: Metastable solid solutions with quartz type structures on the join $SiO_2–MgAl_2O_4$. Z. Kristallogr. **116** (1961) p. 60–82.

[24] Bottinga, Y.; Richet, P.: Anorthite, andesine, wollastonite, diopside, cordierite and pyrope: thermodynamics of melting, glass transition, and properties of the amorphous phases. Earth Planet. Sci. Lett. **67** (1984) p. 415–432.

[25] Emde, F.: Tables of higher functions. (In Engl. and German.) Leipzig: Teubner 1952.

[26] Yuritsin, N. S.; Fokin, V. M.; Kalinina, A. M. et al.: Kinetics of crystal nucleation on the surface of cordierite glass. In: Proc. XVI International Congress on Glass, Madrid 1992. Vol. 5. Madrid: Soc. Esp. Ceram. Vid. 1992. p. 21–26. (Bol. Soc. Esp. Ceram. Vid. 31-C (1992) 5.).

Addresses of the authors:
R. Müller, S. Reinsch,
Bundesanstalt für Materialforschung und -prüfung
D-12200 Berlin
W. Pannhorst
Schott Glaswerke
Hattenbergstraße 10, D-55122 Mainz